

Development of simplified discrete limit analysis for three-dimensional slope stability problem

Advantechonology Co.,Ltd.

Eisaku HAMASAKI

Department of Art and Technology, Hosei Univ.,Japan.

Norio TAKEUCHI

Department of Urban and Environmental Engineering, Kyoto Univ.,Japan.

Yuzo OHNISHI

Abstract

In this study, a new simplified discrete limit analysis technique for a three-dimensional slope stability problem is proposed, using divided columns which are three-dimensional elements of RBSM (Rigid Body Spring Model). This approach is easy to use such as the slice method currently used in the conventional slope stability analysis and it helps to develop a very effective slope protection work plan taking into account displacement of each column. In this model, a sliding surface consists of squares, since a column is square. Then, the concept of the isoparametric element is introduced to define this surface. Using this model to analyze a three-dimensional slope stability problem, we showed that the safety factor of a landslide is calculated, and it can predict a movement of the whole body of the slope from combination of displacement direction of each column.

Key Words

slope stability, 3-dimension, RBSM (Rigid Body Spring Model), isoparametric element

1. Introduction

The mainstream of the slope stability analysis for landslides has been the two-dimensional limit equilibrium method, but in the wake of recent advances in computers, the three-dimensional limit equilibrium method, the advanced finite element analysis method, etc. have also been used. However, the three-dimensional finite element analysis requires expertise in setting boundary conditions, specifying physical properties, and it is difficult to interpret results in many cases, so the use of such method is still limited to special cases, when consider the costs and time for analysis.

When we review the recent improvements in the analytical ability of computers, it is certain that the three-dimensional stability analysis of landslides at the level of the limit equilibrium method is not a special analysis but it is now quite common ¹⁾. In addition, at many landslide sites, the geological and topographical conditions have strong influences; for example, the process of forming the slip surface having slickenside was seen at smectite, etc. which was produced at specific areas such as faults, the weathered and altered parts, and the pelitic parts. Namely, it is important for on-site engineers to identify the locations of slip surfaces by investigating the history of the changes in topography, geological characteristics, and landslides. The frequency of utilizing the three-dimensional limit equilibrium method-based slope analysis that assumes that slip surfaces are known is still quite high, compared with three-dimensional numerical analyses, such as the finite element method.

Meanwhile, when an engineer performs three-dimensional stable analysis of a slope, they adopt Hovland's method, which is extension model of two-dimensional Fellenius' method. Hovland's method assumes that the inter-column forces are zero, like the two-dimensional Fellenius' method assumes that the resultant of the internal forces acting on the slice side is parallel with the slip surface (it is ignored, in a strict sense). Therefore, as pointed out by Ugai ³⁾ and Enokida et al. ⁴⁾, Hovland's method difficult to take into account three-dimensional geometric effects such as lateral constraint.

In order to consider three-dimensional geometric effects, Ugai et al. expanded the two-dimensional Janbu's method, Bishop's method, or Spencer's method to the three-dimensional one and assumed that there is a resultant of internal forces acting on the lateral side of column in the direction toward the point of action, to propose an analysis method, etc. ⁵⁾.

However, their a method also needs to make assumptions regarding the point of action of and the direction of the resultant between lateral sides of column, and in the case of three dimensions, a movement direction is set in only one direction on the

horizontal plane to obtain the safety factor. If the movement direction is not determined, it is necessary to obtain the safety factor of the slope by calculating the safety factor for each possible movement direction and seeking the direction of the minimum safety factor⁴⁾.

However, when seeing the displacement directions of observation posts and GPS devices traced in most landslide sites, for example, the landslide in Washiodake⁶⁾, it was often observed that the moving body in a landslide does not move only in one direction. On the other hand, the limit equilibrium model assumes that the hypothetical slide directions of the entire slope are in one direction, to calculate the safety factor, and so there is not a little gap with actual conditions.

In order to solve such problems, the authors adopted the RBSM (Rigid Body-Spring Model), which obtains a discretization equation using the energy stored between elements⁷⁾. RBSM has been developed as a computational model generalizing limit analysis in plasticity. In this model structures or solids are idealized as a set of rigid elements interconnected by two types of spring systems, one of which resists the dilatational deformation, the other, the shearing deformation. Thus, RBSM is so useful for fracture analysis of rock or concrete cracking, which can be regarded as a well-known discrete crack model.

According to this method, by introducing lateral springs that applied the penalty function between the lateral sides of columns, which underwent mesh division on the horizontal plane, it becomes possible to produce a mechanism in which force is transmitted with the displacement of columns, and then it is possible to calculate the safety factor of the slope from the surface force on the slip surface⁸⁾.

The input data used in this method are the same as those for the conventional limit equilibrium method, that is, the unit weight (γt), the cohesion (C), and the internal friction angle (ϕ) of the moving body, and pore water pressure (U). Namely, it becomes possible to obtain the displacement of each column with easy condition-setting, and also to clearly reflect the three-dimensional geometrical effects, especially the lateral constraint condition.

This paper describes the theory and formulation of this method, and with simple model analysis, we show that these three-dimensional stable analysis can consider a restriction effect of landslide's side. And, according to this method, the configuration of a landslide's slip surface is consists of quadrangular, so, we propose a technique of modeling with isoparametric elements.

RBSM の説
明をここで
詳しくのべ
ました

2. Introduction of the Discrete Limit Analysis

2.1 Modeling based on RBSM

In slice methods such as the Hovland's method, the three-dimensional slope is represented by the aggregate of columns (square poles) standing on the X - Y plane, as illustrated in Fig. 2, and the safety factor of each column on the sliding surface is calculated by the limit equilibrium method.

When a discrete limit analysis is conducted under the assumption that these columns are three-dimensional elements of RBSM, the surface force on the sliding surface can be calculated, and the safety factor is calculated from this. The objective of this study is to carry out an analysis easily like a slice method, and a column is defined as an element in RBSM, and the degree of freedom is 3 directions — x , y , and z — to be shown in Fig. 3.

When we cannot constitute slip surface in a quadrangle, in this study, we treat it as the calculation outside. Although generally RBSM considers rotational degree of freedom, this study ignores the deformation of columns and treats the translational movement only, and so rotational displacement is not considered to easily think.

2.2 Formulation for Simplifying Analysis of three-dimensional slope stability problem

(1) Lateral sides of columns

In this study, columns are made in the same way as a conventional division method, so, a calculation of stiffness matrix by RBSM is extremely simplified.

Fig. 4 shows the adjacent element relationship between the x -direction. In this case, the relative displacement on the contact surface A can be calculated with the following equations:

$$\delta = B_x u$$

$$\delta = \{\delta_n \quad \delta_{sx} \quad \delta_{sy}\}^T \quad u = \left\{ u_I \quad v_I \quad \omega_I \mid u_{II} \quad v_{II} \quad \omega_{II} \right\}^T \quad (1)$$

$$B_x = \left[\begin{array}{ccc|ccc} -1 & 0 & 0 & 1 & 0 & 0 \\ 0 & -1 & 0 & 0 & 1 & 0 \\ 0 & 0 & -1 & 0 & 0 & 1 \end{array} \right]$$

Here, u represents the displacement vector, and u , v , ω depict the displacement components in the x , y , and z directions, respectively. The suffixes I and II correspond to the columns shown in Fig. 4.

δ_n , δ_{sx} , and δ_{sy} represent the relative displacements in the normal direction, and the y and z directions, which are perpendicular to the normal direction on the contact surface, respectively, as shown in Equation (1).

In a similar way, the relative displacement δ for the adjacent element in the y direction as shown in Fig. 5 can be calculated with the following equation:

$$\delta = B_y u$$

$$B_y = \left[\begin{array}{ccc|ccc} 0 & -1 & 0 & 0 & 1 & 0 \\ -1 & 0 & 0 & 1 & 0 & 0 \\ 0 & 0 & -1 & 0 & 0 & 1 \end{array} \right] \quad (2)$$

On the other hand, the surface force σ between columns at lateral sides is obtained using the penalty function as follows:

$$\sigma = D_{side} \delta$$

$$\sigma = \{ \sigma_n \quad \tau_{sx} \quad \tau_{sy} \}^T, \quad D_{side} = \begin{bmatrix} \lambda & 0 & 0 \\ 0 & \lambda & 0 \\ 0 & 0 & \lambda \end{bmatrix} \quad (3)$$

Here, σ_n represents the surface force in the vertical direction per unit area on the column's lateral side, and τ_{sx} and τ_{sy} depict the surface force in the shear directions.

Therefore, the energy stored on the columns at lateral side can be calculated by conducting integration on the contact surface A as follows:

$$V_{side} = 0.5 \cdot u^T \int_A B_x^T D_{side} B_x dAu + 0.5 \cdot u^T \int_A B_y^T D_{side} B_y dAu \quad (4)$$

(2) Sliding Surface

As shown in Fig. 6, it is assumed that the sliding surface is given by the following equation:

$$z = z(x, y) \quad (5)$$

At this time, the normal vector can be expressed by the following equation:

$$n = \{ -(\partial z / \partial x) i - (\partial z / \partial y) j + k \} / \sqrt{1 + (\partial z / \partial x)^2 + (\partial z / \partial y)^2} \quad (6)$$

The tangent vectors S_x and S_y in the x and y directions can be calculated in a similar way as follows:

$$S_x = \{ i + (\partial z / \partial x) k \} / \sqrt{1 + (\partial z / \partial x)^2} \quad (7)$$

$$S_y = \{ j + (\partial z / \partial y) k \} / \sqrt{1 + (\partial z / \partial y)^2}$$

Here, the displacement vector u of the column can be expressed by the following equation with the unit vectors in the x , y , and z directions— i , j , and k .

$$u = ui + vj + wk \quad (8)$$

At this time, the relative displacement δ_n , δ_{sx} , and δ_{sy} on the sliding surface can be calculated as follows under the assumption that there is no movement of the bedrock.

$$\delta_n = u \cdot n, \delta_{sx} = u \cdot s_x, \delta_{sy} = u \cdot s_y \quad (9)$$

Consequently, the following relation can be obtained.

$$\delta = Bu$$

$$B = \begin{bmatrix} -(\partial_z/\partial_x)/L & -(\partial_z/\partial_y)/L & 1/L \\ 1/L_x & 0 & (\partial_z/\partial_x)/L_x \\ 0 & 1/L_y & (\partial_z/\partial_y)/L_y \end{bmatrix} \quad (10)$$

$$L = \sqrt{1 + (\partial_z/\partial_x)^2 + (\partial_z/\partial_y)^2}, L_x = \sqrt{1 + (\partial_z/\partial_x)^2}, L_y = \sqrt{1 + (\partial_z/\partial_y)^2}$$

When the relation between the relative displacement and surface force on the sliding surface is expressed as follows:

$$\sigma = D\delta, \quad D = \begin{bmatrix} \lambda n & 0 & 0 \\ 0 & \lambda_{sx} & 0 \\ 0 & 0 & \lambda_{sy} \end{bmatrix} \quad (11)$$

the energy on the sliding surface (contact surface A) can be estimated with the following equation:

$$V_{slip} = 0.5 \cdot u^T \int_A B^T D B dA u \quad (12)$$

Here, D represents the matrix of the spring of the penalty (λ).

Therefore, the energy of the entire system becomes as follows:

$$V = V_{side} + V_{slip} \quad (13)$$

By deriving a discrete equation from this relation, it becomes possible to conduct a three-dimensional discrete analysis based on RBSM.

2.3 Gradient of the Sliding Surface

As mentioned in the previous section, the equation representing the sliding surface: $z = z(x, y)$ is defined using bilinear isoparametric quadrangle elements, and then the gradient of the sliding is calculated⁹⁾. Fig. 7 shows one example of the shape function of this element, and there is the following relation between the natural coordinate system and the physical coordinate system.

$$x(\xi, \eta) = \sum_{\alpha=1}^4 N_{\alpha}(\xi, \eta) x_{\alpha}, \quad y(\xi, \eta) = \sum_{\alpha=1}^4 N_{\alpha}(\xi, \eta) y_{\alpha} \quad (14)$$

Here, N_{α} represents the shape function. Since α is the quadrangle element, α is equal to 1 to 4. As for isoparametric elements, physical quantities are interpolated using the same shape function as coordinate transformation. Here, the z -coordinate is considered as the physical quantity, and an area is defined with the following equation:

$$z(x, y) = z(x(\xi, \eta), y(\xi, \eta)) = \sum_{\alpha=1}^4 N_{\alpha}(\xi, \eta) z_{\alpha} \quad (15)$$

At this time, the gradient of the sliding surface can be expressed by the following equation:

$$\begin{Bmatrix} \partial z / \partial x \\ \partial z / \partial y \end{Bmatrix} = \begin{bmatrix} \partial \xi / \partial x & \partial \eta / \partial x \\ \partial \xi / \partial y & \partial \eta / \partial y \end{bmatrix} \begin{Bmatrix} \partial z / \partial \xi \\ \partial z / \partial \eta \end{Bmatrix} = J^{-1} \begin{Bmatrix} \partial z / \partial \xi \\ \partial z / \partial \eta \end{Bmatrix} \quad (16)$$

Here, J represents a Jacobian matrix. By substituting Equations (14)-(16) into Equation (7), it is possible to calculate the normal vector and gradient of the rectangular surface (Fig. 8). Therefore, the gradient of the sliding can be obtained for each integration point by means of numerical integration.

In this study, an integration point is set at a central point, and the gradient at this central point is defined as the gradient of the sliding surface. In the natural coordinate system, the central point becomes $(\xi, \eta) = (0, 0)$, and equal to the normal vector that is derived from the midpoint vectors in the x and y directions on the rectangular area.

2.4 Weight and Head Height of the Column

By defining the intersection of the two lines that are drawn by connecting the weight and head height of the column, and the central point of the column's bottom on the x - y plane, that is, the midpoint of the diagonal line, as the representative point, the average of the height components is calculated.

Therefore, as for a square pole, the following equations are used as shown in Fig. 9.

- Altitude of the column's ground level (Ht)

$$Ht = (Zt_1 + Zt_2 + Zt_3 + Zt_4) / 4 \quad (17)$$

- Altitude of the column's groundwater level (Hw)

$$Hw = (Zw_1 + Zw_2 + Zw_3 + Zw_4) / 4 \quad (18)$$

- Altitude of the column's sliding surface (Hb)

$$Hb = (Zb_1 + Zb_2 + Zb_3 + Zb_4) / 4 \quad (19)$$

- Column's weight (W)

Assuming that the unit weight is (γt),

$$W = \Delta X \cdot \Delta Y \cdot \Delta t (Ht - Hb) \quad (20)$$

- Head height of the column's center (U)

$$U = Hw - Hb \quad (21)$$

In this method, when adding the weight term to water pressure including pore water pressure, the body force acts on the sliding surface and the column's lateral side in the perpendicular direction to each surface at the head height. Accordingly, the surface force on the sliding surface is the outcome after summing up all acting forces including the pore water pressure.

2.5 Entire Safety Factor

When RBSM-based discrete analysis is conducted, the normal force (N) and tangent forces (T_x, T_y) on the sliding surface of each column is obtained. In this analysis, the safety factor is calculated from these surface forces with the following equation:

$$F_s = \frac{\sum \{ \tan \phi \cdot N + C \cdot A \}}{\sqrt{(\sum T_x)^2 + (\sum T_y)^2}} \quad (22)$$

$$= R / D$$

Here, ϕ represents the internal friction angle of the sliding surface, C represents the cohesion, and A depicts the area of the sliding surface. In addition, the numerator R represents the shear strength resisting the sliding, and the denominator D depicts the reluctant of the shear strengths on the sliding surface.

3. Sensitivity Analysis of Lateral Constraint Pressure and Landslide Configuration Ratio

In this section, the effects of constraint pressure are clarified utilizing this method. With regard to the landslide configuration and the safety factor, a model is developed based on the relation between width (w) and thickness (d) (which is the ratio of “ w/d ” here) and an analysis is attempted. For comparison, the simplified three-dimensional Janbu's and Hovland's methods are also used for analysis.

3.1 Analysis Conditions

As analysis conditions, the two three-dimensional models (a) and (b) shown in Figs. 10 and 11 were prepared. In addition, Fig. 12 shows the cross sections of the models. Model (a) has a steep crest and a gentle foot like an ordinary landslide, not only its lateral sides, while Model (b) has a homogeneous slope that does not show any change in gradient from its crest to foot. Such a setting was conducted with the purpose of describing clearly the lateral constraint. Here, it was assumed that the gradient of the homogeneous slope is $\tan \theta = 0.3$ ($\theta = 16.7^\circ$), and Cases 1 to 5 in Table 1 were analyzed.

In addition, in order to discuss the difference in the internal friction angle ϕ , $\phi =$

20° and $\phi = 10^\circ$ were assumed in Cases 1 and 2, respectively, where the same analysis model was used for Cases 1 and 2. Moreover, the three models of landslide thickness of 12 m, 27 m, and 54 m were used for Cases 1, 3, and 4, respectively for the sensitivity analysis with respect to the landslide thickness (d).

In Cases 1, 2, and 5, it was assumed that the grid widths “ dx ” and “ dy ” are both 2.5 m, and in Case 3, the grid width was 5.0 m, and in Case 4, it was 10.0 m. The “ $W2$ ” of the bottom surface of the sliding surface shown in Fig. 12 was calculated with the equation: $W2 = W - 2 \cdot dx$. Moreover, to directly grasp the constraint condition of this method, the work of the column located at $(i, j) = (29, 22)$, in the right side of the center of landslide of Model (b), Case 5, per m^2 in the x direction, was calculated by multiplying the displacement of the column in the x direction and the surface force in the x direction (Fig. 13). Here, i and j represent the column numbers in the x and y directions, respectively.

3.2 Analysis Results

In Fig. 14, the results of each case are plotted with the vertical axis being the safety factor (F_s) and the horizontal axis being the w/d ratio, where “RBSM” represents the safety factor obtained in the simplified three-dimensional safety analysis model, “Janbu” represents the safety factor in the simplified three-dimensional Janbu’s method, and “Hovland” depicts the safety factor in Hovland’s method. In addition, Fig. 15 shows the relation between the safety factor of RBSM of Case 5 of Model (b) and the work of the column near the center of the landslide region ($i = 29, j = 22$) in the x direction. From the above analysis results, the following characteristics were found:

- (1) RBSM and Janbu decrease exponentially as the w/d ratio increases. When the w/d ratio is small, RBSM is higher than Janbu. However, when w/d is 2 or larger, the decrease behaviors of both are almost the same. On the other hand, Hovland does not depend on w/d and is nearly constant, excluding Cases 2 and 3, but in Cases 2 and 3, the rate of change of Hovland is small compared with Janbu and RBSM.
- (2) In Model (b), which has no effects of edge configurations such as foot and crest, there are no differences in safety factor between this method and the simplified three-dimensional Janbu’s method. On the other hand, in Model (a), the safety factor in this method tends to be higher (constraint effect is stronger) than that in the simplified three-dimensional Janbu’s method.
- (3) From the comparison between Cases 1 and 2, it was found that RBSM and Janbu become higher as ϕ increases and they decrease in the same way as the w/d ratio

increase. When Cases 1, 3, and 4, whose ϕ are the same and whose d are different from one another, are compared, the change in safety factor at a small w/d becomes smaller as d is thicker, but there are no significant differences among Cases, and $w/d = 7-10$, and the safety factor is constant.

- (4) In Model (a), when the w/d ratio exceeds 7-10, Hovland and Janbu become almost the same. In addition, in Model (b), Janbu and RBSM are nearly equal to each other.

3.3 Discussion of Constraint Condition Analysis

With regard to discussions on the configuration, scale, and stability of landslides, there is an old report by Watari et al.¹⁰⁾, and Ueno also focused on the relation between the landslide's maximum width (W) and the depth of the sliding surface (D) at a landslide site he investigated, calculated the cross dimensional ratio " W/D " with a simplified equation, demonstrated that the safety factor becomes almost constant when W/D is 10 or larger, and provided a logical explanation for the result that $W/D = 3.0-10.7$, which was obtained at the site he studied¹¹⁾.

Also in the analysis of this study, RBSM and Janbu become constant suddenly when the w/d ratio exceeds 7-10. In addition, the fact that the work in the x direction, which is shown in Fig. 15, becomes almost zero when the w/d ratio exceeds 11 demonstrates that the same configuration effects as the w/d ratio of Ueno et al. work. The reason why RBSM is slightly higher than Janbu in Model (a) while they are equal in Model (b) is considered to be that the configuration of the changing points of the sliding surface gradient in the vertical direction causes considerable constraint effects in the analysis of RBSM. In addition, from the comparison between Cases 1 and 2, it can be said that the lateral constraint effect is not considerably large when seeing the w/d ratio.

Although Hovland changes slightly when the w/d ratio of Cases 2 and 3 in Fig. 14 is 3 or lower, Hovland does not change in Case 5. This is because the gradient of the sliding surface is not homogeneous but twisted at the columns of both edges of the landslide and the gradient becomes gentler at the edges. Therefore, the analysis result of Hovland became as if there were the constraint effects.

Anyway, it was found that this analysis, in which the limit discretization method of RBSM is used, considers the effects of the landslide configuration to a sufficient degree, and that this method shows larger vertical constraints and a higher safety factor than Janbu's method.

4. Analysis Cases

As mentioned in the previous section, it is a fact that the landslide movement direction varies on the surface of the moving body, according to the observation of moving pegs.

In the reports of Kishita⁶⁾ and Rou¹²⁾, the landslide of Washio-dake shown in Fig. 1 shows the three-dimensional topology and sliding surface, and so the stability analysis with this method was attempted based on them. The location of groundwater was estimated three-dimensionally based on the high water¹²⁾ and the flow distribution map⁶⁾. In addition, considering that there exists basalt above an altitude of 210 m, the landslide moving body has a two-layered structure: layers of basalt and of other substances. Then, it was assumed that the unit weight of the soil mass of the former (γ) is 27 kN/m³ and that of the latter is 26 kN/m³. With regard to cohesion (C) and internal friction angle (ϕ), it was assumed that $C = 16.4$ kPa and $\phi = 21.7^\circ$, which are the results of the ring shear test, in Case 1, and that $C = 16.4$ kPa and $\phi = 11.35^\circ$, from which $F_s = 1.0$ is obtained via the back calculation with this method (RBSM), in Case 2.

The Hovland's method and the simplified three-dimensional Janbu's method were compared in safety factor. The direction of the minimum safety factor in each method was defined as the clockwise angle from the downward y axis. The results are shown in Table 2. As for Case 2 based on this method, the direction of the column's movement (solid line) and the maximum gradient of the column (dashed line) are shown in Fig. 16.

Table 2 states that the safety factor obtained in the present method indicates the highest value like the sensitivity analysis mentioned previously. However, in the previous section, Janbu becomes almost equal to Hovland as the w/d ratio becomes higher, but according to research records, the safety factor obtained in the simplified three-dimensional Janbu's method is higher. This is endorsed by the study of the collapse of Ontake by Ugai³⁾ in which the safety factor in the simplified three-dimensional Janbu's method is higher than that in Hovland's method. In the present analysis (RBSM), the safety factor becomes further higher than that in the simplified three-dimensional Janbu's method. This is considered to be because the present analysis considers not only the lateral sides but also the vertical direction in discussing the displacement due to the three-dimensional configuration effects. In addition, when comparing the direction of the column's movement shown in Fig. 16 and the moving pegs shown in Fig. 1, it is found that although there are some differences in the movement direction at the east edge and central part of the head part of the landslide, the movement directions from the western edge to the end of the landslide and Peg No. 11 are the same.

5. Conclusion

The proposed method is based on the discretization limit analysis method similar to RBSM, and differs from the conventional Hovland's method and simplified three-dimensional Janbu's method. A good point of this method is gathered to four following items.

- 1) With this method, it is possible to obtain a safety factor taking into account each column's displacement.
- 2) In addition, the three-dimensional configuration effects could not be described by Hovland's method, but the present method induces the lateral constraint like the simplified three-dimensional Janbu's method and higher constraints in the direction of the sliding surface than the simplified three-dimensional Janbu's method. And therefore the safety factor becomes higher as a whole.
- 3) Anyway, the present analysis method can conduct comparison with the movement directions, according to the analysis of the case of the landslide at Washio-dake, and it can be found from such data that the present method is one of the clues to judging the stability of the sliding surface structure.
- 4) And, this method is almost the same as the conventional limit equilibrium method in necessary parameters, assumed landslide structures, and analysis time, and so the easiness in carrying out analysis is retained.

-----5.結論-----

提案した手法は、RBSMと同様の離散化極限解析手法に基づいたもので、従来のHovland法や三次元簡易Janbu法と異なっている。この解析の利点は以下の3点に集約される。

- 1) 個々のカラム変位(移動)を考慮した安全率が得られる手法である。
- 2) さらに、三次元形状効果は、従来いわれていたようにHovland法ではほとんど示すことができなかったが、本手法は側方拘束において三次元簡易Janbu法と遜色なく、またすべり方向で見ると三次元簡易Janbu法より大きな拘束をもたらし、全体に安全率も高めに推移することが分かった。
- 3) いずれにしても、本解析手法は、鷲尾岳地すべりの事例解析でも、移動方向との比較が可能であることを明らかにしており、このようなデータから、すべり面構造の是非を判断する手段となり得る手法の一つであることが分かる。
- 4) また、本手法では、必要とする地盤定数や地すべり面構造の設定及び解析時間が従来手法の極限平衡法とほぼ同じであり、処理のための簡便性が失われない方法である。

References

- 1) Takatoshi Kimura, Kouji Kawaba (2000): On the Preventive Construction Method Plan based on Three-Dimensional Stability Analysis, the Lecture Record of the 39th Conference of the Japan Landslide Society, pp. 253-256
- 2) Hovland, H. J., Asce, M. (1977): Three-Dimensional Slope Stability Analysis Method, Journal of the Geotechnical Engineering Division, pp. 971-986
- 3) Keizou Ugai (1988): Discussion of the Three-Dimensional Stability of Slopes with the Decomposition Method, Soil and Fundamentals, Vol. 36, No. 5, pp. 19-24
- 4) Mitsuya Enokida (2003): Discussion on Lateral Wall Effects and Movement Directions Using the Simplified Three-Dimensional Janbu Method, the Lecture Record of the 42nd Conference of the Japan Landslide Society, pp. 177-180
- 5) Keizou Ugai, Kenji Hosomizo (1988): Three-Dimensional Extension of the Simplified Bishop Method, the Simplified Janbu Method, and the Spencer Method, the Journals of the Japan Society of Civil Engineers, Issue No. 394/III-9, pp. 21-26
- 6) Shinitzu Kinoshita, Hizuki Tanaka, Tetsuya Sakai, Hiroyuki Yoshimatsu (2001): Three-Dimensional FEM Analysis Case of Deep Pegs at Landslide Sites, Landslide, Vol. 38, No. 3, pp. 268-275
- 7) Norio Takeuchi (1991): Discretization Limit Analysis in Ground Mechanics, Baifuukan, pp. 1-204
- 8) Norio Takeuchi, Eisaku Hamasaki, Morito Kusabuka (2003): Simplified Slope Stability Analysis Using Finite Elements, Transactions of the Japan Society for Computational Engineering and Science, Vol. 8, No. 2, pp. 567-570
- 9) Eisaku Hamasaki, Norio Takeuchi, Morito Kusabuka (2003): Three-Dimensional Slope Stability Analysis Approximating the Sliding Surface with Finite Elements, the Lecture Record of the 38th Conference of the Japan Landslide Society, pp. 3-4
- 10) Masasuke Watari, Hiroyuki Nakamura, Osamu Itagaki (1975): Statistics of the Actual Conditions of Landslides (Part 1), Reference from Public Works Research Institute, pp. 6-34
- 11) Masashi Ueno (2001): Discussion of Topographic and Geological Factors in Constraining the Configurations and Scale of Landslide, Landslide, Vol. 38, No. 2, pp. 1-10
- 12) Yu-Hua Lang, Hirohuki Nakamura (2003): Three-Dimensional Stability Analysis of a Landslide at Washiodake and the Stress Distribution of Deep Pegs, the Lecture Record of the 42nd Conference of the Japan Landslide Society, pp. 317-320

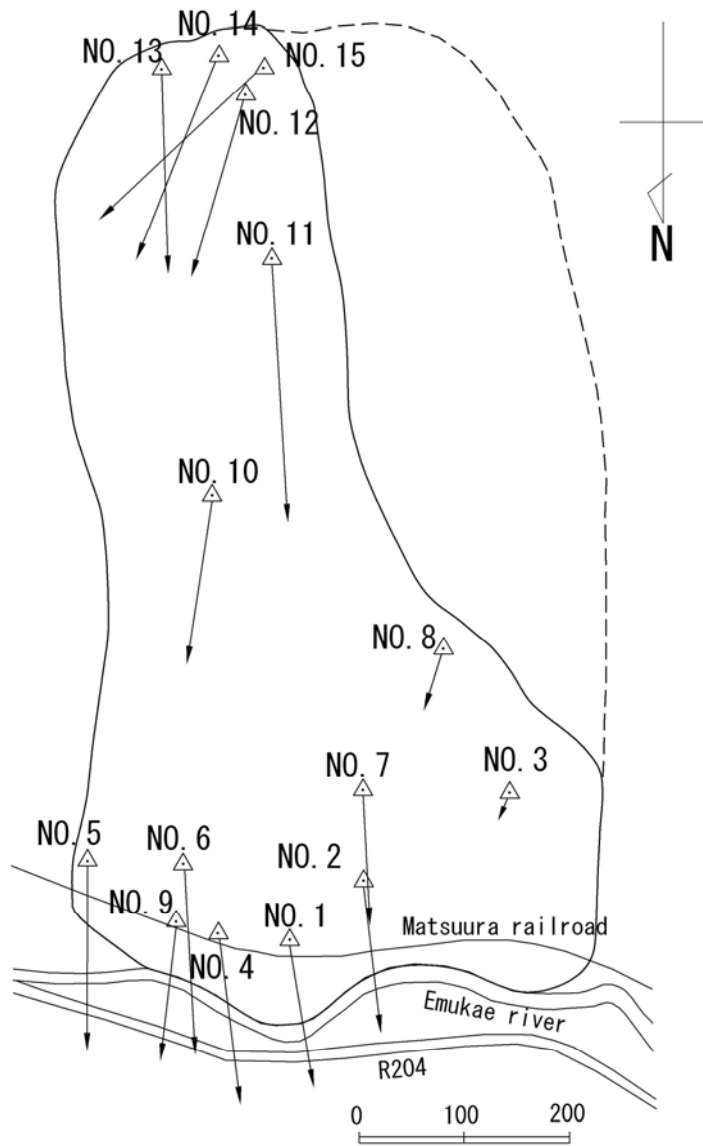


Fig. 1 Movement direction of observation posts in Washiodake landslide area
 (Kinoshita, 2001) ⁶⁾

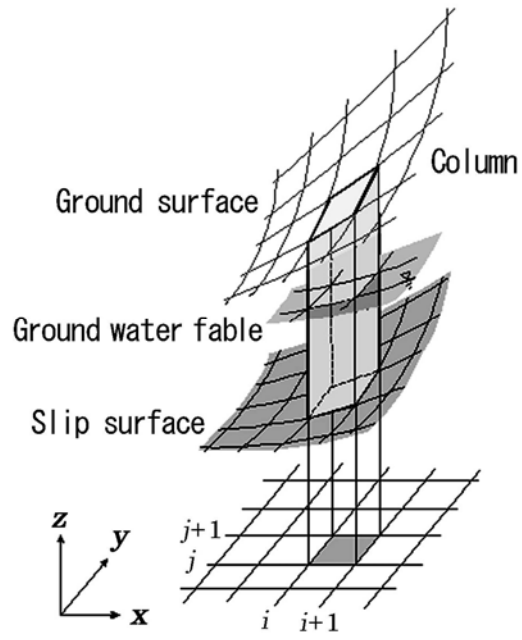


Fig. 2 3-dimensional discretization of sliding body by using columns

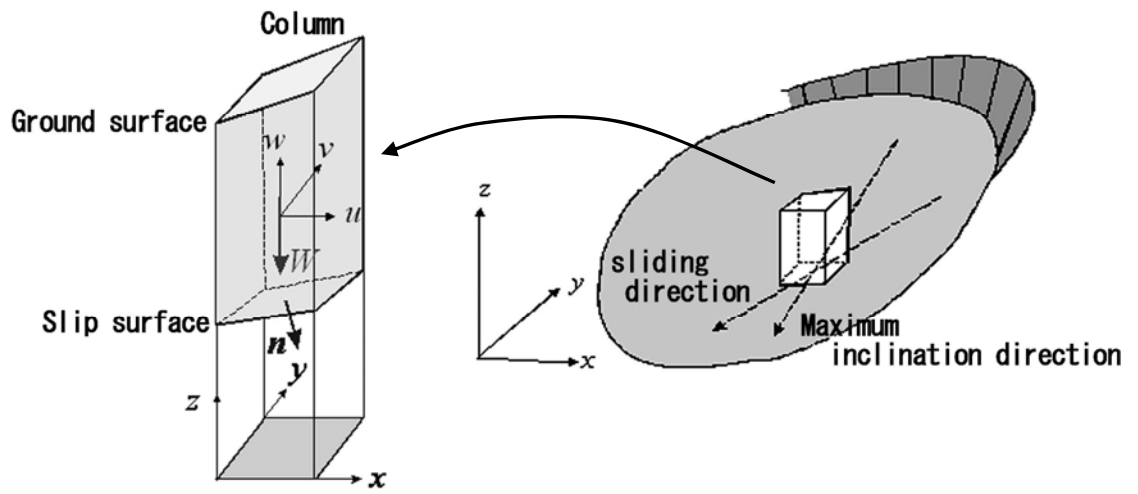


Fig. 3 Degree of freedom for a column.

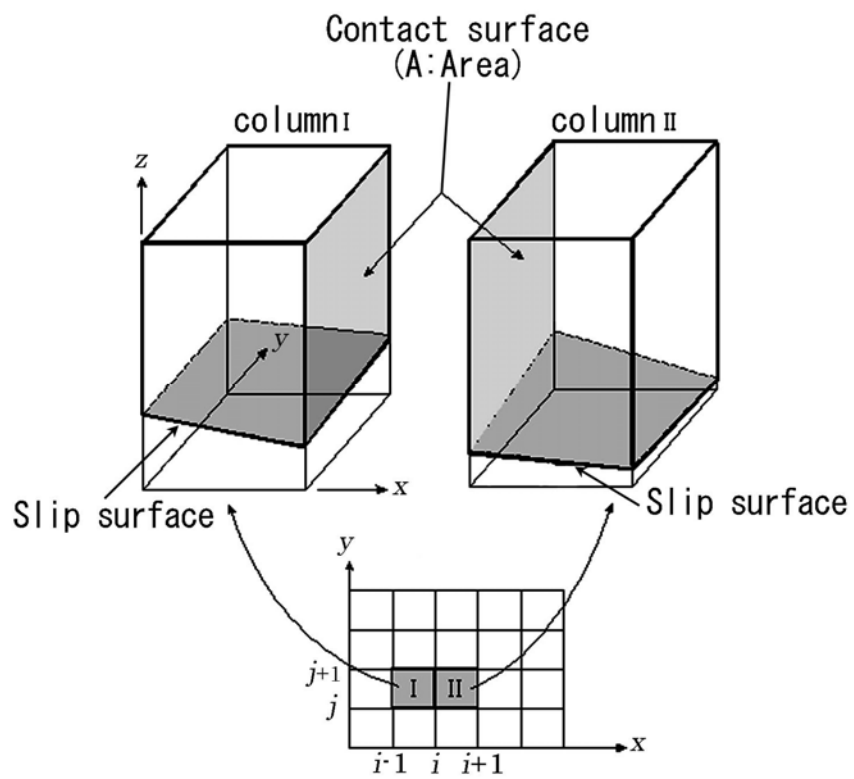


Fig. 4 Contact condition of columns in X-direction

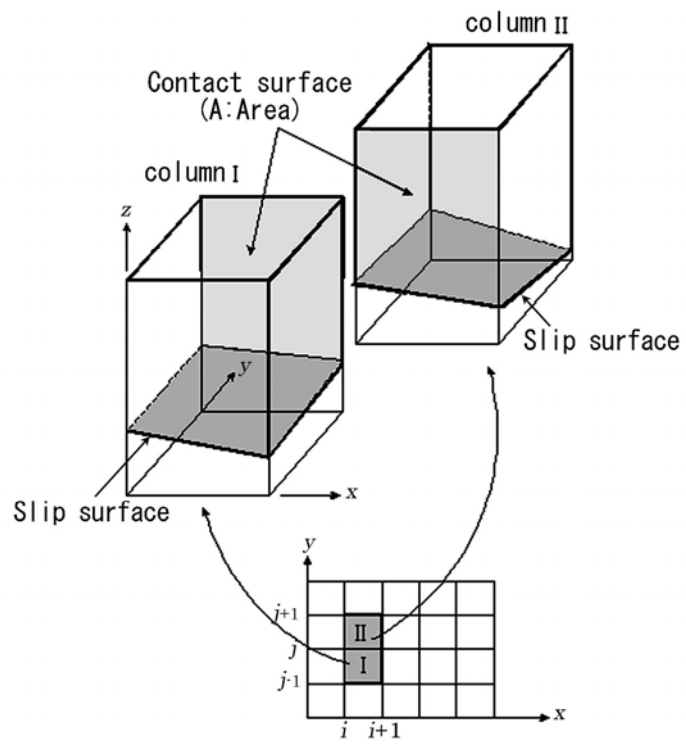


Fig. 5 Contact condition of columns in Y-direction

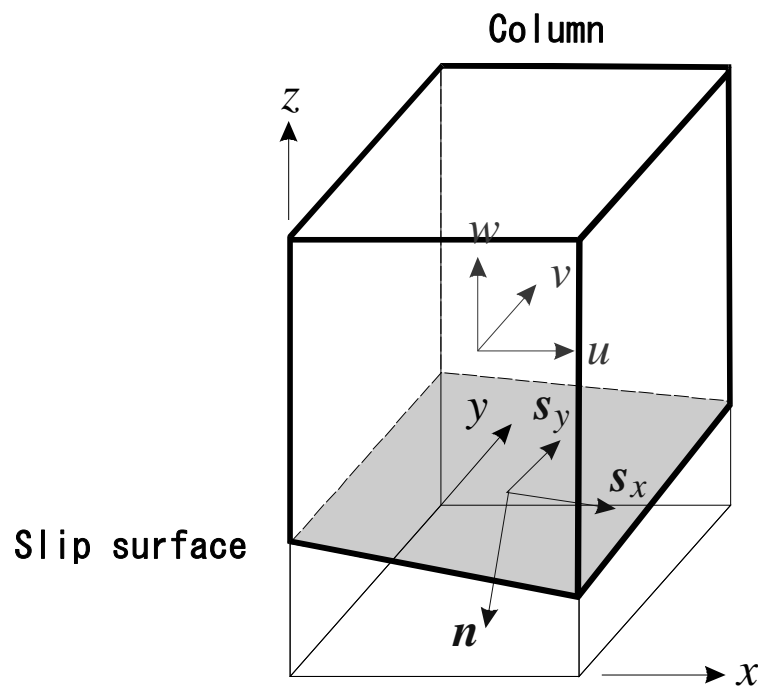


Fig.6 Normal vector and its direction at a sliding surface

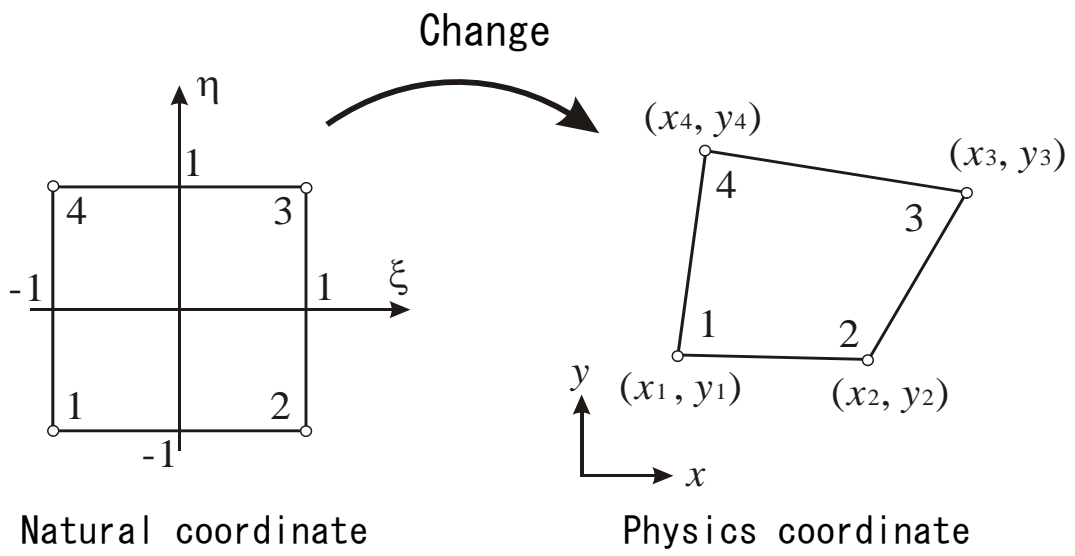


Fig.7 Isoparametric element for a quadrilateral area

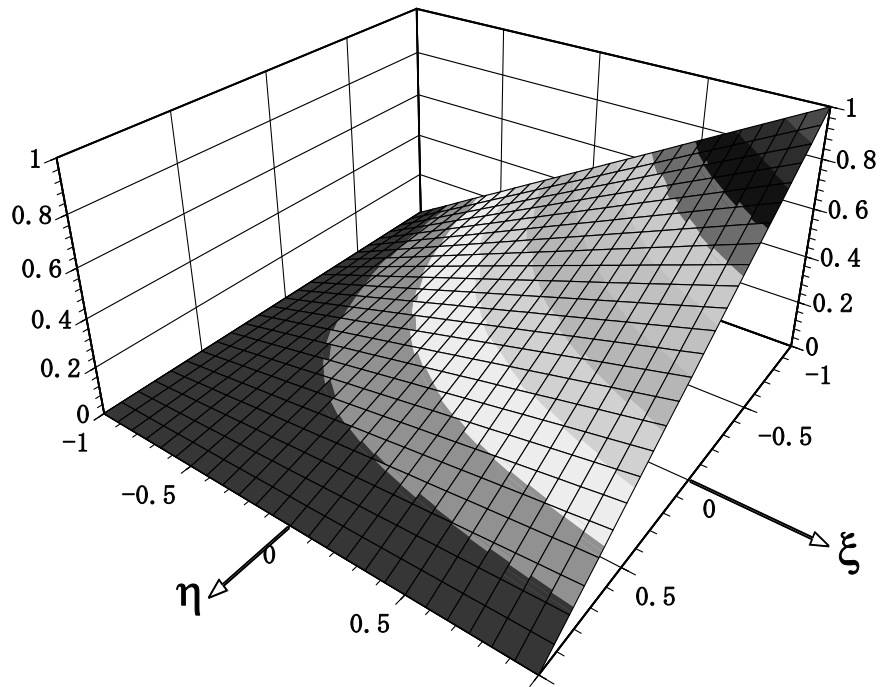


Fig. 8 An example of shape function

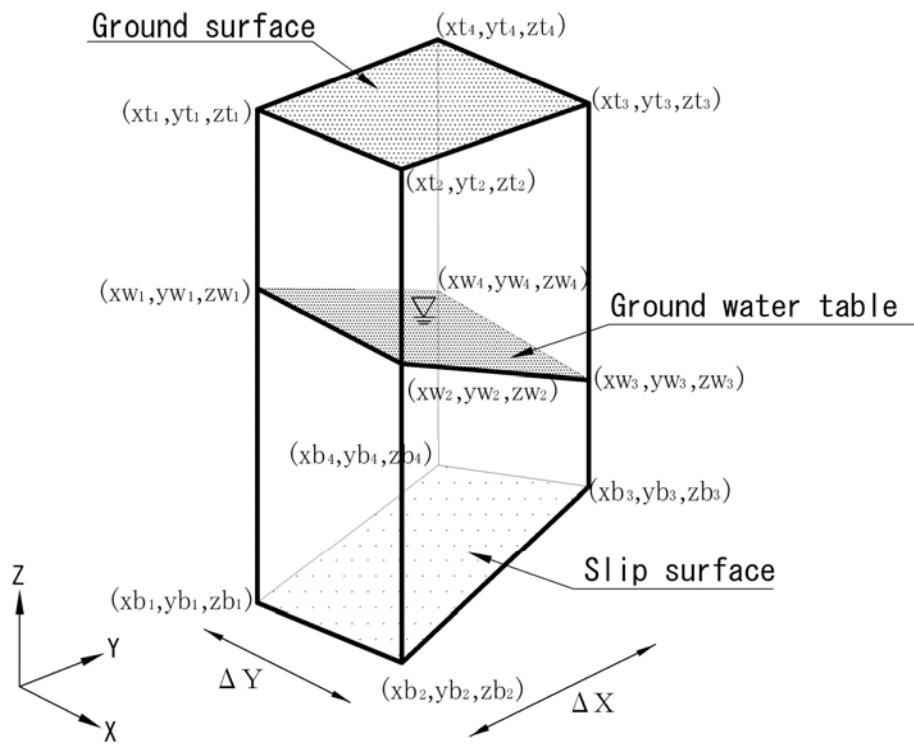


Fig. 9 Coordinate to calculate weight of a column and water head

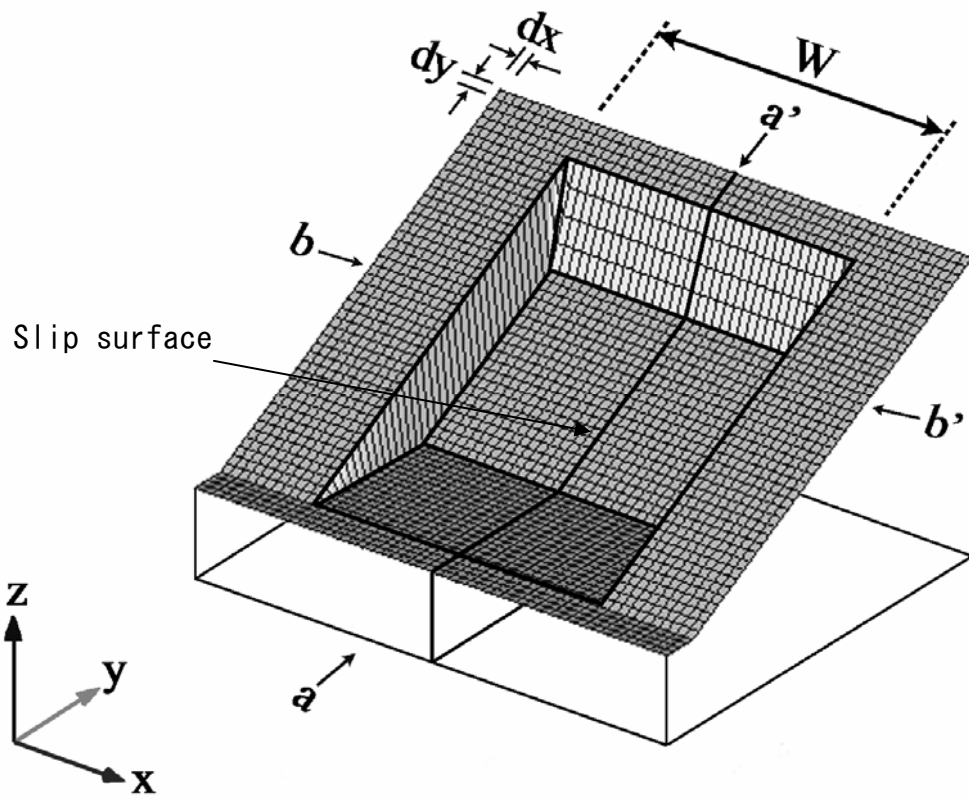


Fig. 10 Schematic view of landslide model (model a)

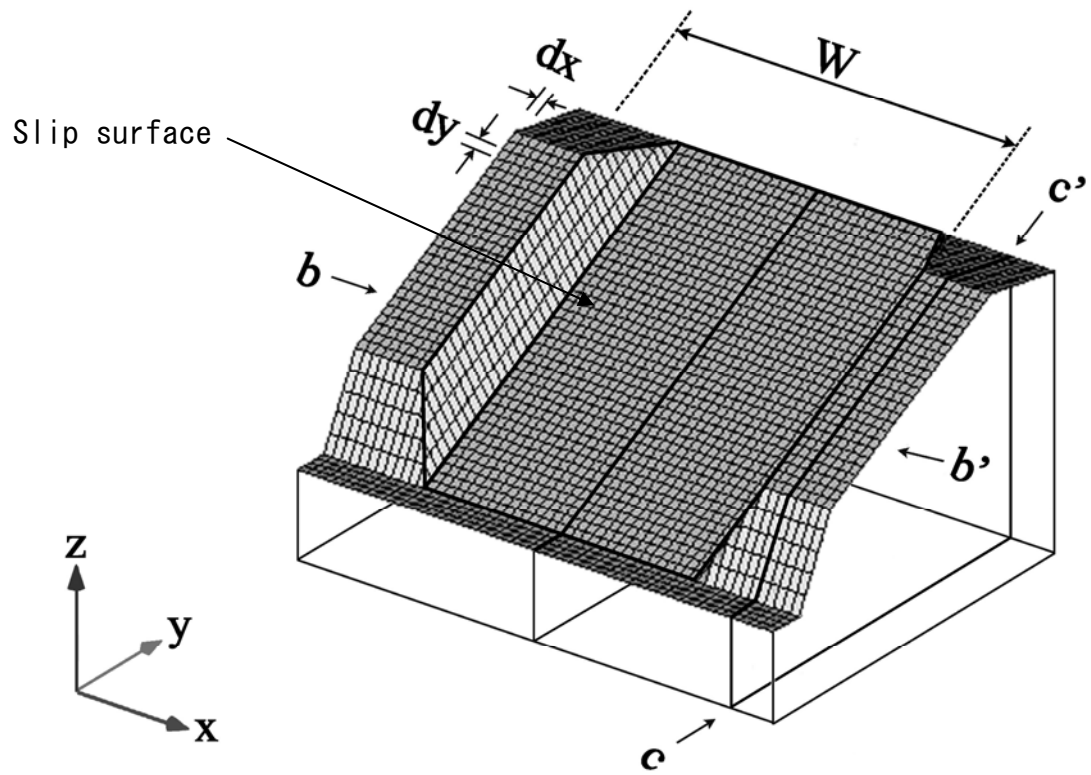


Fig. 11 Schematic view of landslide model (model b)

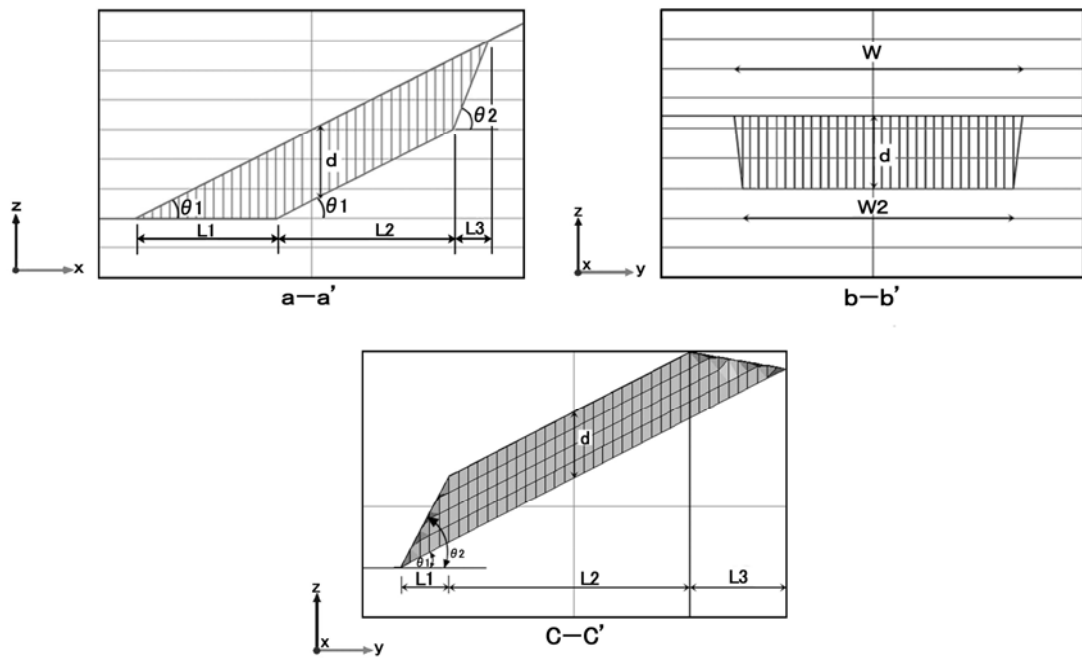


Fig. 12 Cross sections of the landslide model

Table 1 Parameters used in calculation models

Case	Model	C kPa	ϕ °	γt kN/m ³	w m	L1 m	L2 m	L3 m	d m	tan θ 1	tan θ 2
1	a	10	20	18	20 - 130	40	50	10	12	0.3	1.5
2	a	10	10	18	20 - 130	40	50	10	12	0.3	1.5
3	a	10	20	18	20 - 190	90	100	11.25	27	0.3	1.5
4	a	10	20	18	40 - 520	180	210	45	54	0.3	1.5
5	b	10	20	18	30 - 120	12.5	75	25	20	0.3	1.9

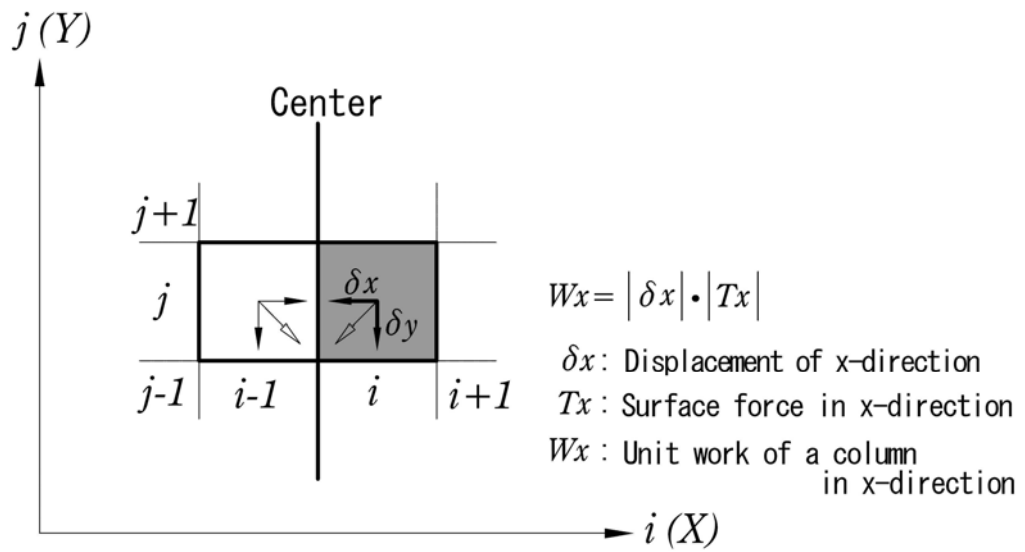
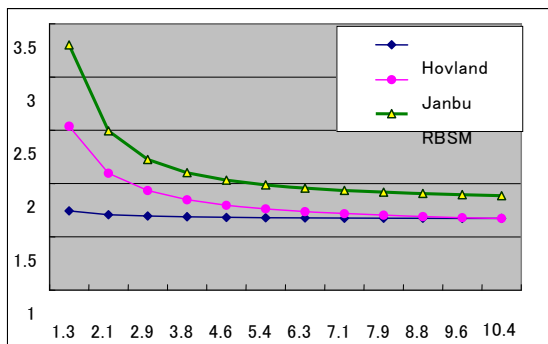
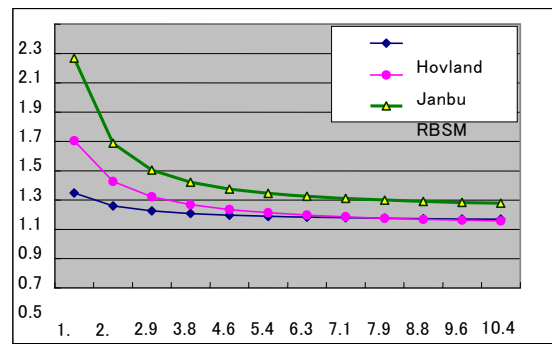


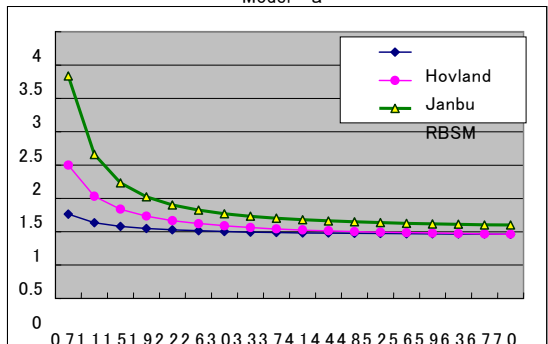
Fig. 13 Unit work of a column in X-direction



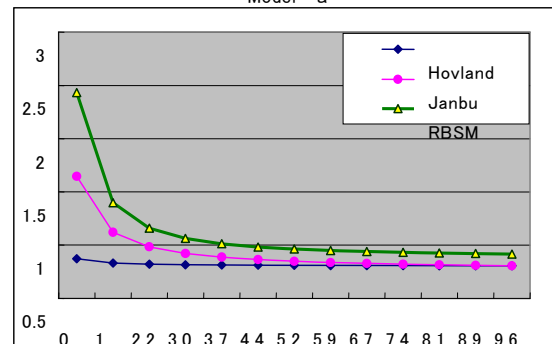
Case1 (d=12m, $\phi = 20^\circ$)
Model a



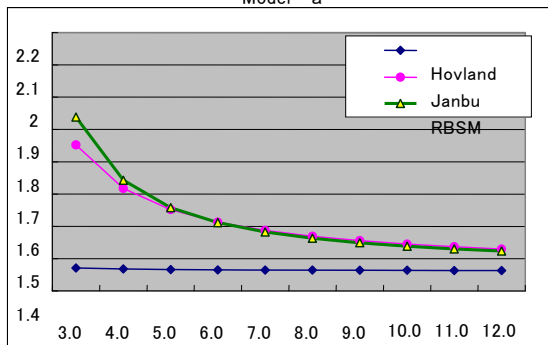
Case2 (d=12m, $\phi = 10^\circ$)
Model a



Case3 (d=27m, $\phi = 20^\circ$)
Model a



Case4 (d=54m, $\phi = 20^\circ$)
Model a



Case5 (d=10m, $\phi = 20^\circ$)
Model b

Horizontal axis : Ratio of W/d
Vertical axis : Safety factor (Fs)

Fig. 14 Relations between safety factors by various methods with ratio of width (w) and thickness (d) of landslide

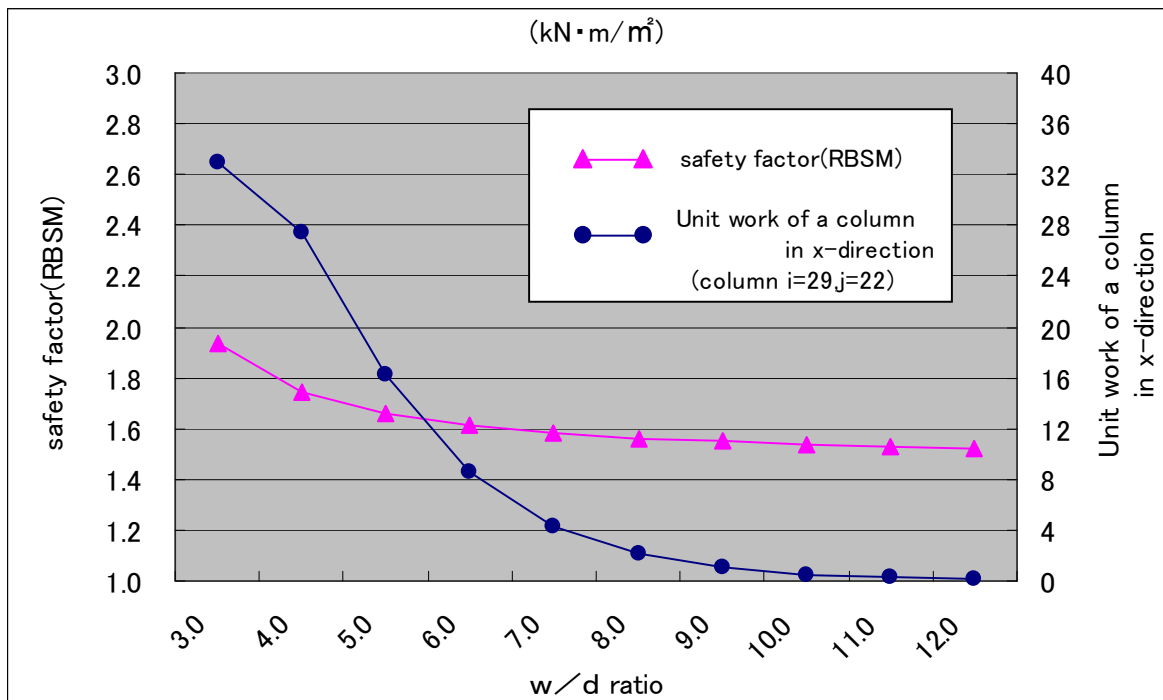


Fig. 15 Relations between w/d ratio versus safety factor by RBSM and unit work in X direction

Table 2 Comparison for safety factors and movement directions between RBSM, Janbu method and Hovland method at Washiodake area

Case	Condition	Safety factor (Three dimensions method)		
		RBSM	Janbu's method	Hovland's method
①	C=16.40kPa, $\phi=21.70^\circ$	1.88	1.66 (3°)	1.53 (10°)
②	C=16.40kPa, $\phi=11.35^\circ$	1.00	0.89 (3°)	0.83 (10°)

※() is sliding direction of minimum safety factor.

And, 0° is North direction and proceeds around watch.

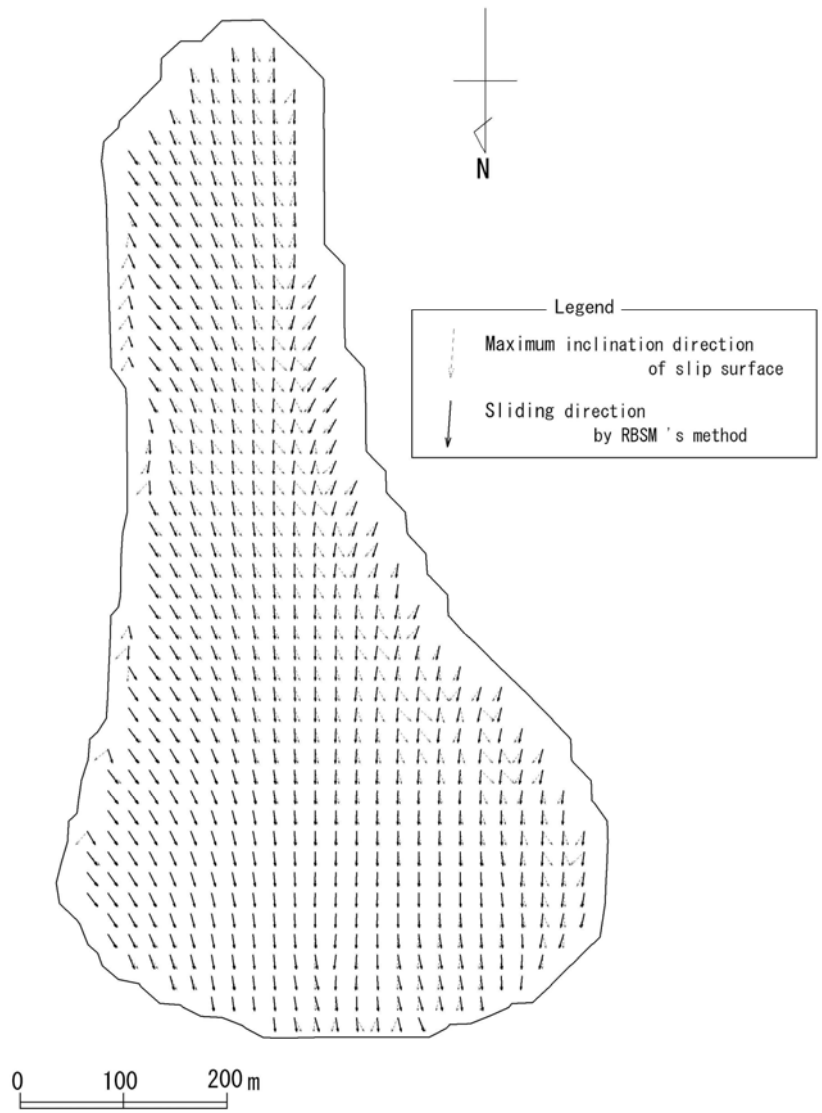


Fig. 16 Comparison of calculated movement direction of column and maximum inclination direction using by RBSM.

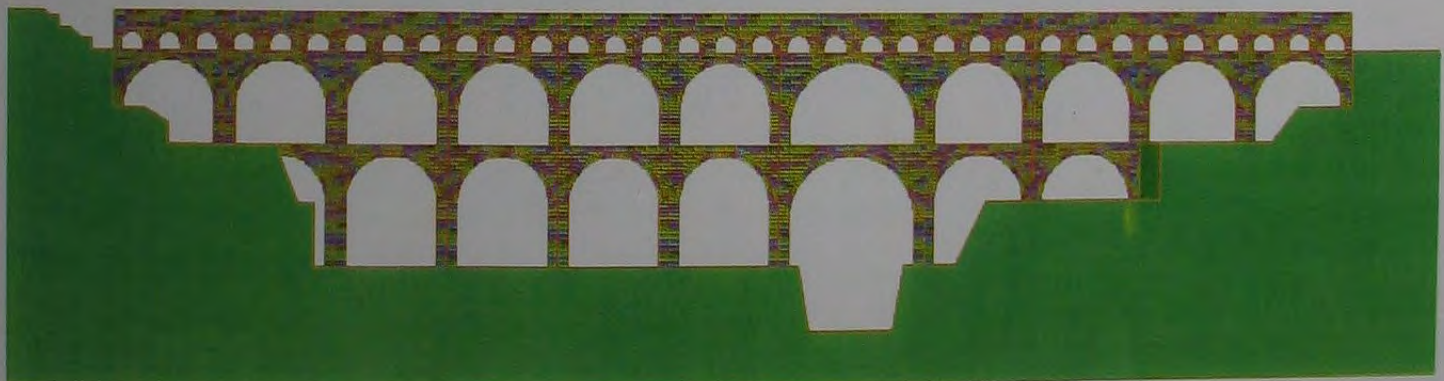
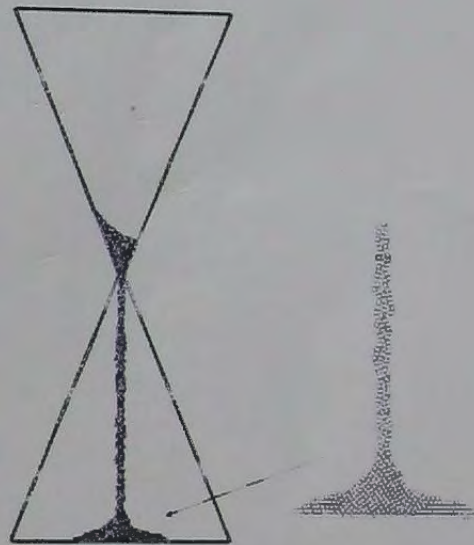
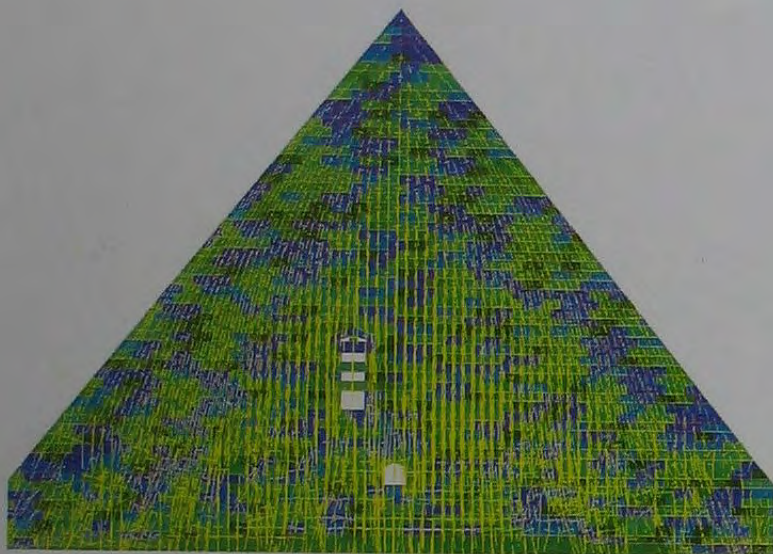
PROCEEDINGS OF

International Mini-Symposium for Numerical Discontinuous Analyses

- The 20th anniversary of Japanese society for
discontinuous analyses-

November 21, 2008

Kona, *Hawaii*



Proceedings Compiled & Edited by

Yuzo Ohnishi and Tomofumi Koyama, Kyoto University